

Thermal Brownian motor

This article has been downloaded from IOPscience. Please scroll down to see the full text article.

2005 J. Phys.: Condens. Matter 17 S3673

(<http://iopscience.iop.org/0953-8984/17/47/002>)

View [the table of contents for this issue](#), or go to the [journal homepage](#) for more

Download details:

IP Address: 129.252.86.83

The article was downloaded on 28/05/2010 at 06:48

Please note that [terms and conditions apply](#).

Thermal Brownian motor

P Meurs and C Van den Broeck

Hasselt University, B-3590 Diepenbeek, Belgium

Received 3 August 2005

Published 4 November 2005

Online at stacks.iop.org/JPhysCM/17/S3673

Abstract

Recently, a thermal Brownian motor was introduced (Van den Broeck *et al* 2004 *Phys. Rev. Lett.* **93** 090601), for which an exact microscopic analysis is possible. The purpose of this paper is to review some further properties of this construction, and to discuss in particular specific issues including the relation with macroscopic response and the efficiency at maximum power.

1. Introduction

Brownian motors are small-scale engines that operate on the basis of nonequilibrium fluctuations. Most of the models that have been discussed previously in the literature refer to the transfer of chemical or potential energy into work [1] by Brownian entities that operate in an externally imposed asymmetric environment (or by spontaneous symmetry breaking [2]). In this case, 100% efficiency can in principle be achieved [3], in accordance with the basic laws of thermodynamics. Recently, a thermal Brownian motor was introduced [4], for which an exact microscopic analysis turns out to be possible [5]. The model can be viewed as a simplification of the Feynman–Smoluchowski ratchet [6, 7]. This construction differs in two essential aspects from most other Brownian motors. First, the source of energy is the presence of different heat baths. Thermodynamics thus predicts that the limiting efficiency is that of the Carnot engine. Second, the asymmetry is an intrinsic property of the motor, not of the environment or of the imposed constraint. The purpose of this paper is to review some further properties of this construction, and to discuss in particular specific issues including the relation with macroscopic response and the efficiency at maximum power.

2. Model and basic results

We first briefly review the basic construction of the thermal Brownian motor and the main results. The motor consists of a set of convex units i ($i = 1, \dots, N$), that move as a rigidly linked entity with a single degree of freedom along a specified direction x . Each unit resides in a separate, infinitely large compartment that is filled with an ideal gas at equilibrium. These compartments play a role akin to the thermal reservoirs in a Carnot construction. For simplicity, we consider the case of spatial dimension $d = 2$ with coordinates (x, y) . In figure 1 we show

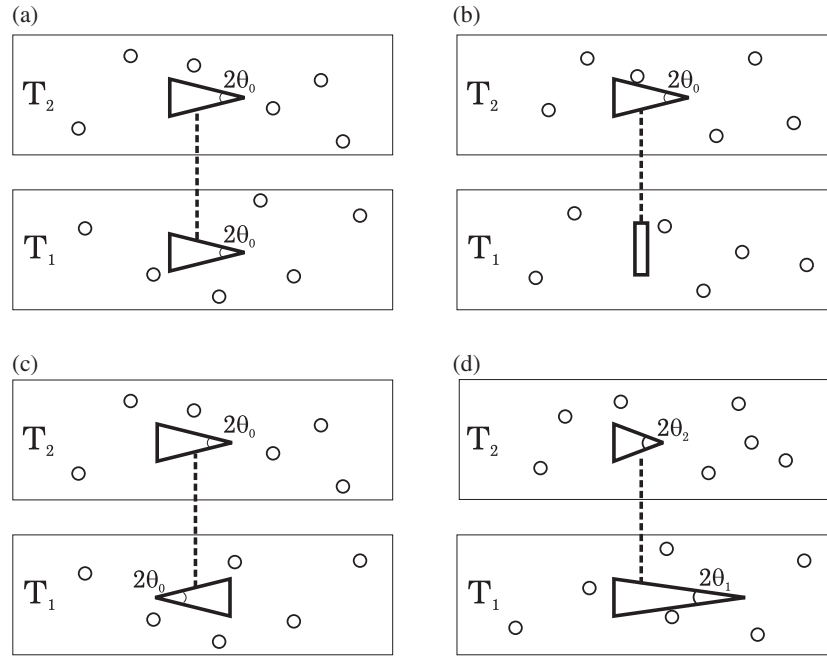


Figure 1. Four different realizations of the thermal Brownian motor, each consisting of two rigidly linked motor units. Model (a) will be referred to as Triangula and is composed out of two identical triangles, while model (b) is called Triangulita and has a triangle and a bar. Constructions (c) and (d) consist respectively of two identical triangles pointing in the opposite direction and two triangles with a different apex angle.

four different realizations of the motor. The gas particles are point particles of mass m . Their density, temperature and Maxwellian velocity distribution in compartment i are denoted by ρ_i , T_i and ϕ_i , respectively, with

$$\phi_i(v_x, v_y) = \frac{m}{2\pi k_B T_i} \exp\left(\frac{-m(v_x^2 + v_y^2)}{2k_B T_i}\right). \quad (1)$$

We consider the limit in which the mean free path of the gas particles is much larger than the linear dimension of the motor unit. In this case, there are no pre-collisional correlations between the speed of the motor and that of the impinging particles. The probability density $P(V, t)$ for the speed $\vec{V} = (V, 0)$ therefore obeys a Boltzmann–Master

$$\frac{\partial P(V, t)}{\partial t} = \int dV' [W(V|V')P(V', t) - W(V'|V)P(V, t)]. \quad (2)$$

$W(V|V') = \sum_i W_i(V|V')$ is the transition probability per unit time for the motor to change speed from V' to V due to the collisions with the gas particles in the compartments $i = 1, \dots, N$. Its explicit form, following from the collision rules and basic arguments from kinetic theory, is given by (see [5] for more details)

$$W_i(V|V') = \int_0^{2\pi} d\theta S_i F_i(\theta) \int_{-\infty}^{+\infty} dv'_x \int_{-\infty}^{+\infty} dv'_y \rho_i \phi_i(v'_x, v'_y) (\vec{V}' - \vec{v}') \cdot \hat{e}_\perp \\ \times \Theta[(\vec{V}' - \vec{v}') \cdot \hat{e}_\perp] \delta\left[V - V' - \frac{2\frac{m}{M} \sin^2 \theta}{1 + \frac{m}{M} \sin^2 \theta} (v'_x - v'_y \cot \theta - V')\right]. \quad (3)$$

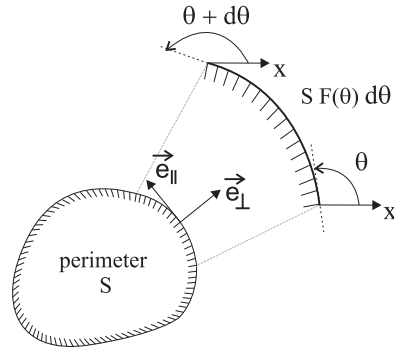


Figure 2. A closed and convex object with perimeter S . The length of the surface with an orientation between θ and $\theta + d\theta$ is $S F(\theta) d\theta$, defining the form factor $F(\theta)$.

Here Θ is the Heaviside step function. The δ Dirac function selects appropriate particle velocities yielding the post-collisional speed V for the motor in function of the pre-collisional speeds V' and v'_x, v'_y of motor and gas particle respectively. The shape of the motor unit i is characterized by a normalized shape function $F_i(\theta)$, such that $F_i(\theta) d\theta$ is the fraction of the outer surface of the unit that has a tangent between θ and $\theta + d\theta$, see figure 2. The angle θ is measured counterclockwise from the horizontal x direction. The total perimeter will be denoted by S_i .

Solving the Boltzmann–Master equation in general is out of the question, even at the steady state. To make progress, a perturbative solution is necessary. Since we expect that the rectification disappears in the limit of a macroscopic motor, a natural expansion parameter is the ratio of the mass m of the gas particle over the mass M of the object. More precisely, we have used $\varepsilon = \sqrt{m/M}$ as the expansion parameter.

Introducing the transition probability $W_i(V'; r) = W_i(V|V')$ with jump amplitude $r = V - V'$, the Boltzmann equation can be rewritten as

$$\frac{\partial P(V, t)}{\partial t} = \int W(V - r; r) P(V - r, t) dr - P(V, t) \int W(V; -r) dr. \quad (4)$$

The Taylor expansion of the rhs of this equation with respect to the jump amplitude leads to the equivalent Kramers–Moyal expansion:

$$\frac{\partial P(V, t)}{\partial t} = \sum_{n=1}^{\infty} \frac{(-1)^n}{n!} \left(\frac{d}{dV} \right)^n \{a_n(V) P(V, t)\}, \quad (5)$$

with jump moments $a_n(V) = \sum_i a_{n,i}(V)$, defined as

$$a_{n,i}(V) = \int r^n W_i(V; r) dr. \quad (6)$$

One can obtain from the Kramers–Moyal expansion the set of coupled equations for the moments of the velocity distribution $\langle V^n \rangle = \int V^n P(V, t)$. Of interest for the subsequent discussion, we reproduce the exact results for the first two moment equations:

$$\partial_t \langle V \rangle = \langle a_1(V) \rangle \quad (7)$$

$$\partial_t \langle V^2 \rangle = 2 \langle V a_1(V) \rangle + \langle a_2(V) \rangle, \quad (8)$$

with

$$\begin{aligned}
a_{1,i}(V) = & -\rho_i S_i \int_0^{2\pi} d\theta F_i(\theta) \frac{1}{M + m \sin^2 \theta} \\
& \times \left[\sqrt{\frac{2k_B T_i m}{\pi}} \exp\left[-\frac{m}{2k_B T_i} V^2 \sin^2 \theta\right] V \sin^2 \theta \right. \\
& \left. + \left(1 + \operatorname{erf}\left[\sqrt{\frac{m}{2k_B T_i}} V \sin \theta\right]\right) (k_B T_i \sin \theta + m V^2 \sin^3 \theta) \right] \quad (9)
\end{aligned}$$

$$\begin{aligned}
a_{2,i}(V) = & 2\rho_i S_i \int_0^{2\pi} d\theta F_i(\theta) \frac{\sin^2 \theta}{(M + m \sin^2 \theta)^2} \\
& \times \left[\sqrt{\frac{2k_B T_i m}{\pi}} \exp\left[-\frac{m}{2k_B T_i} V^2 \sin^2 \theta\right] (2k_B T_i + m V^2 \sin^2 \theta) \right. \\
& \left. + \left(1 + \operatorname{erf}\left[\sqrt{\frac{m}{2k_B T_i}} V \sin \theta\right]\right) (3k_B T_i m V \sin \theta + m^2 V^3 \sin^3 \theta) \right]. \quad (10)
\end{aligned}$$

3. Systematic speed: general results

The equation for the first moment is coupled to the higher moments, a familiar feature in statistical mechanics. However, a perturbative solution can be obtained by considering the Taylor expansion in ε . To lowest order in ε the first moment equation reduces to a closed equation featuring a linear relaxation law, namely

$$M \partial_t \langle V \rangle = -\gamma \langle V \rangle, \quad (11)$$

where $\gamma = \sum_i \gamma_i$ and γ_i is the linear friction coefficient, due to the section of the motor sitting in gas mixture i :

$$\gamma_i = 4\rho_i S_i \sqrt{\frac{k_B T_i m}{2\pi}} \int_0^{2\pi} d\theta F_i(\theta) \sin^2 \theta. \quad (12)$$

Note that, at this level of the perturbation, the steady-state speed of the motor is zero: even though the motor may be constituted of asymmetric parts, no rectification takes place at the level of linear response.

At the next order in the perturbation, the first moment is coupled to the second one, which needs to be solved at lowest order. By doing so, one finds, at the steady state,

$$M \langle V^2 \rangle = k_B T_{\text{eff}}, \quad (13)$$

with T_{eff} the effective temperature given by

$$T_{\text{eff}} = \frac{\sum_i \gamma_i T_i}{\sum_i \gamma_i}. \quad (14)$$

By inserting this result in the equation for the average velocity, one finds for the lowest order term of the steady-state velocity V_0

$$V_0 \equiv \langle V \rangle = \sqrt{\frac{m}{M}} \sqrt{\frac{\pi k_B T_{\text{eff}}}{8M}} \frac{\sum_i \rho_i S_i \left(\frac{T_i}{T_{\text{eff}}} - 1\right) \int_0^{2\pi} d\theta F_i(\theta) \sin^3 \theta}{\sum_i \rho_i S_i \sqrt{\frac{T_i}{T_{\text{eff}}}} \int_0^{2\pi} d\theta F_i(\theta) \sin^2(\theta)}. \quad (15)$$

This speed is equal to the expansion parameter times the thermal speed of the motor and further multiplied by a factor that depends on the geometric properties of the object. Note that the Brownian motor ceases to function in the absence of a temperature difference (when $T_i = T_{\text{eff}}$

Table 1. Analytic result for the lowest-order contribution to $\langle V \rangle$ for the different constructions depicted in figure 1.

Shape	Fig.	Stationary velocity V_0 (order ε)
Triangula	1(a)	$\frac{\sqrt{2\pi k_B m}}{4M} (1 - \sin \theta_0) \frac{\rho_1 \rho_2 (T_1 - T_2) (\sqrt{T_1} - \sqrt{T_2})}{[\rho_1 \sqrt{T_1} + \rho_2 \sqrt{T_2}]^2}$
Triangulita	1(b)	$\frac{\sqrt{2\pi k_B m}}{4M} (1 - \sin^2 \theta_0) \frac{2\rho_1 \rho_2 \sqrt{T_1} (T_1 - T_2)}{[2\rho_1 \sqrt{T_1} + \rho_2 \sqrt{T_2} (1 + \sin \theta_0)]^2}$
Triangle–triangle ($\triangleright \triangleleft$)	1(c)	$\frac{\sqrt{2\pi k_B m}}{4M} (1 - \sin \theta_0) \frac{\rho_1 \rho_2 (T_1 - T_2) (\sqrt{T_1} + \sqrt{T_2})}{[\rho_1 \sqrt{T_1} + \rho_2 \sqrt{T_2}]^2}$
Triangle–triangle ($\theta_1 \neq \theta_2$)	1(d)	$\frac{\sqrt{2\pi k_B m}}{4M} \frac{\rho_1 \rho_2 (1 + \sin \theta_1) (1 + \sin \theta_2) (T_1 - T_2) [\sqrt{T_1} (1 - \sin \theta_2) - \sqrt{T_2} (1 - \sin \theta_1)]}{[\rho_1 \sqrt{T_1} (1 + \sin \theta_1) + \rho_2 \sqrt{T_2} (1 + \sin \theta_2)]^2}$

for all i) and in the macroscopic limit $M \rightarrow \infty$ (since $V_0 \sim 1/M$). Note also that the speed is scale independent, i.e., independent of the actual size of the motor units: V_0 is invariant under the rescaling S_i to CS_i . In table 1 we have collected the explicit result for V_0 for the four different thermal motors, depicted in figure 1.

It is tempting to interpret the direction of the systematic speed on the basis of intuition. One can study the response of the motor by the application of an external force. Due to the asymmetry, the response curve (speed versus force) will be asymmetric. In particular, it will require less force to move a triangle in the ‘easy’ direction of the sharp angle. Consequently, one expects that fluctuations leading to an ‘extra force’ in the easy direction would be more successful in moving the object than the ones in the other direction. A similar argument can be applied to the discussion of the electric current in a diode, which also has an asymmetric response of current versus field. One expects that fluctuations in the electric field will produce a larger current in one direction than in the other one. However, as is well known [8], these arguments are clearly wrong. The first observation is that there is no systematic speed (or electric current) when the system is at equilibrium. In fact, the effect of possible asymmetries in a system are completely wiped out in equilibrium, as expressed explicitly in the principle of detailed balance discovered by Onsager [9]: at equilibrium any process and its time-reverse occur equally frequently. Second, equilibrium is typically a so-called point of flux reversal [7]. For example, in the case of Triangulita, the flux is in the ‘easy’ direction of the sharp angle only in the case when the temperature is lower in the reservoir containing the triangle. Otherwise the speed is in the opposite direction. Furthermore the speed again becomes zero when the temperature is zero in the reservoir containing the flat paddle. Finally, the above-mentioned asymmetry in the response appears in the nonlinear regime. In this regime, the dynamics of the various moments are however coupled. In particular, the equation for the average speed is not closed, but depends on the entire probability distribution. The nonlinear response to an external force is therefore not linked in an obvious way to the intrinsic nonlinear dynamics generated by nonequilibrium fluctuations.

Full information on the equation of the first moment is contained in the nonlinear function $a_{1,i}(V)$. It is reproduced in figures 3(a) and (b) for the motor units used in the constructions of figure 1. However, the direction of motion, to lowest order in ε , contains much less information. Indeed, from equation (15), one finds, for a motor with 2 units,

$$\text{sgn}(V_0) = \text{sgn} \left[(T_1 - T_2) \left(\frac{\langle \sin^3 \theta \rangle_1}{\langle \sin^2 \theta \rangle_1} - \sqrt{\frac{T_1}{T_2}} \frac{\langle \sin^3 \theta \rangle_2}{\langle \sin^2 \theta \rangle_2} \right) \right]. \quad (16)$$

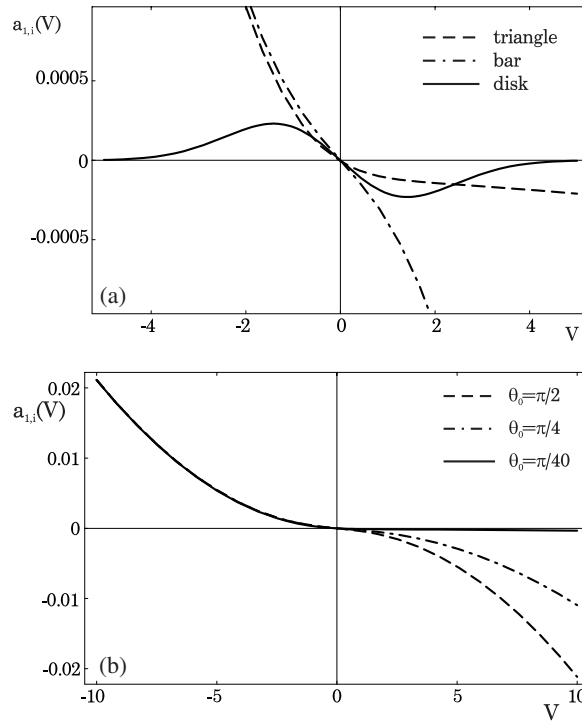


Figure 3. (a) Top: the response function $a_{1,i}(V)$, see equation (9), for different geometric objects used in the constructions of figure 1: a triangle with $\theta_0 = \pi/36$, a bar of length L and a disc with radius R . (b) Bottom: the function $a_{1,i}(V)$ for a triangle with opening angle respectively equal to π , $\pi/2$ and $\pi/20$. The following parameter values were used: mass ratio $M/m = 20$, density $\rho_i = 0.0022$, temperature $T_i = 1$, size $L = R = 1$ and $k_B = 1$ by choice of units.

Hence the direction of the average speed does not depend on the densities of the gases or the size of the motor units. The quantity $-1 \leq \langle \sin^3 \theta \rangle_i = \int_0^{2\pi} d\theta F_i(\theta) \sin^3 \theta \leq 1$ is a measure for the sharpness of the unit:

$$\langle \sin^3 \theta \rangle \begin{cases} \rightarrow 1 & \text{infinitely sharp to the left} \\ = 0 & \text{symmetric upon reflection about } y\text{-axis} \\ \rightarrow -1 & \text{infinitely sharp to the right.} \end{cases} \quad (17)$$

On the other hand the quantity $0 \leq \langle \sin^2 \theta \rangle \leq 1$ is proportional to the linear friction coefficient, see equation (12). For a bar of zero width, it has the minimal value $\langle \sin^2 \theta \rangle = 0$ when the bar is oriented horizontally, while it is maximal ($\langle \sin^2 \theta \rangle = 1$) for a vertical bar.

Based on equation (16), one can distinguish four different classes of motor, depending on how the direction of speed is affected upon interchanging the temperatures T_1 and T_2 . The examples of figure 1 each represent one such class. Figure 4 illustrates their behaviour upon switching T_1 and T_2 .

4. Systematic speed: special cases

To gain further insight on the direction of the systematic speed, it is instructive to calculate its explicit value for a number of special cases; see also table 1.

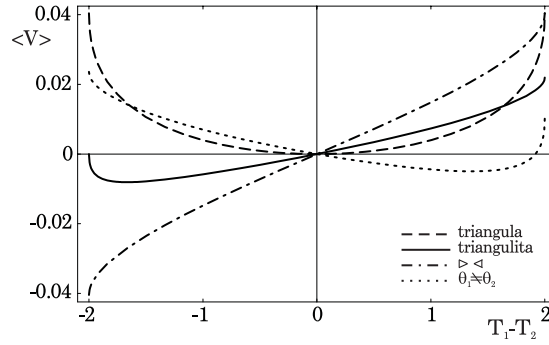


Figure 4. Plot of the average speed (see table 1) for the four different models depicted in figure 1 as a function of the applied temperature difference. The following parameter values are used: $M/m = 20$, $\rho_1 = \rho_2 = 0.0022$, $\theta_0 = \pi/36$, $\theta_1 = \pi/1000$, $\theta_2 = \pi/3$ and $T_1 + T_2 = 2$ fixed.

4.1. Identical units and nonlinear response

For a construction with identical motor units, see for example Triangula (figure 1(a)) with two triangles pointing in the same direction, equation (16) reduces to $\text{sgn}(V_0) = \text{sgn}(-\langle \sin^3 \theta \rangle)$. One concludes that the direction of Triangula's motion is independent of the temperature gradient. This behaviour originates from the permutational symmetry of the identical motor units, implying that the speed must be invariant under the interchange of T_1, ρ_1 with T_2, ρ_2 . Note that the average velocity is pointing in the direction of the sharp angle of the motor units. It turns out that this feature is general: for a motor with two identical units, equation (15) simplifies to

$$V_0 = \frac{\sqrt{2\pi mk_B}}{4M} \rho_1 \rho_2 \frac{(T_1 - T_2)(\sqrt{T_1} - \sqrt{T_2}) \langle \sin^3 \theta \rangle}{[\rho_1 \sqrt{T_1} + \rho_2 \sqrt{T_2}]^2 \langle \sin^2 \theta \rangle}. \quad (18)$$

We conclude that the motion is always in the same direction, the 'easy' direction determined by the sign of $\langle \sin^3 \theta \rangle$; see equation (17).

We again stress that while the above direction of motion appears to be plausible, in agreement with our intuition, this specific feature is exceptional and a result of the permutation symmetry of the units. In fact, the latter symmetry has a dramatic effect on the response of the motor to the temperature gradient: as is clear from equation (18), the speed has a parabolic profile in function of the applied temperature difference $T_1 - T_2$. In particular there is no linear response regime, with a speed proportional to $T_1 - T_2$! It is due to this unusual, symmetry-induced property that equilibrium is not a point of flux reversal.

4.2. Identical units, with opposite orientation

Another interesting class of motor is those with identical units, but pointing in opposite directions; see figure 1(d). For these motors $F_1(\theta) = F_2(\pi - \theta)$ and consequently

$$\langle \sin^n \theta \rangle_1 = \begin{cases} \langle \sin^n \theta \rangle_2 & n \text{ even} \\ -\langle \sin^n \theta \rangle_2 & n \text{ odd.} \end{cases} \quad (19)$$

One finds from equation (15) that the average velocity is given by

$$V_0 = \frac{\sqrt{2\pi mk_B}}{4M} \rho_1 \rho_2 \frac{(T_1 - T_2)(\sqrt{T_1} + \sqrt{T_2}) \langle \sin^3 \theta \rangle_1}{[\rho_1 \sqrt{T_1} + \rho_2 \sqrt{T_2}]^2 \langle \sin^2 \theta \rangle_1}. \quad (20)$$

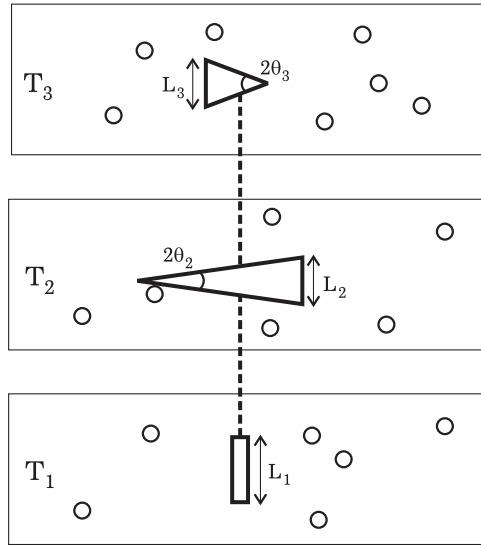


Figure 5. Construction of a thermal Brownian motor with three reservoirs. The three motor units are rigidly linked and move as one single entity.

We conclude that the equilibrium state $T_1 = T_2$ is the (only) point of flux reversal. In the particular case of equal density ($\rho_1 = \rho_2$), we have a symmetric Brownian motor, i.e. the absolute value of its speed is invariant upon inverting the temperature gradient; see [10].

4.3. Different units

When the shape of the two motor units is different, the situation can be quite more involved. In particular, there may be multiple points of flux reversal as a function of the applied temperature difference. This reinforces the statement that the direction of motion is difficult to predict. As an explicit example, we show in figure 4 that a construction with two different triangles (figure 1(d)) has a second reversal point for $T_1 \gg T_2$.

4.4. Multiple reservoirs

To illustrate the effect of multiple reservoirs on the amplitude and direction of the speed, we consider the case with three units, namely two triangles (with different orientation and apex angle) and a bar; see figure 5. The stationary velocity reads

$$\begin{aligned}
 V_0 = & \frac{\sqrt{2\pi mk_B}}{4M} \frac{1}{\left[2\rho_1 L_1 \sqrt{T_1} + \rho_2 L_2 (1 + \sin \theta_2) \sqrt{T_2} + \rho_3 L_3 (1 + \sin \theta_3) \sqrt{T_3}\right]^2} \\
 & \times \left\{ \rho_2 (1 - \sin^2 \theta_2) \left[2\rho_1 L_1 \sqrt{T_1} (T_2 - T_1) + \rho_3 L_3 (1 + \sin \theta_3) \sqrt{T_3} (T_2 - T_3)\right] \right. \\
 & \left. + \rho_3 (\sin^2 \theta_3 - 1) \left[2\rho_1 L_1 \sqrt{T_1} (T_3 - T_1) + \rho_2 L_2 (1 + \sin \theta_2) \sqrt{T_2} (T_3 - T_2)\right] \right\}. \quad (21)
 \end{aligned}$$

The speed is of the same order of magnitude as before. The net motion disappears at equilibrium ($T_1 = T_2 = T_3$), when the asymmetry vanishes ($\theta_2 = \theta_3 = 0$, both triangles are flat), or when the effect of the two units cancels each other (for example $\theta_2 = \theta_3$, $T_2 = T_3$ and $\rho_2 = \rho_3$,

i.e., both have the same opening angle in a reservoir at the same temperature and with equal density).

One may wonder what is the effect of the addition of a reservoir that is at equilibrium with a motor consisting of two units (at lowest order in ε). More precisely, consider T_1 to be equal to the effective temperature of reservoirs 2 and 3, $T_1 = (\gamma_2 T_2 + \gamma_3 T_3)/(\gamma_2 + \gamma_3)$. We find from equation (15)

$$V_0 = \frac{\sqrt{2\pi mk_B}}{4M} \frac{\rho_2 S_2 (T_2 - T_1) \langle \sin^3 \theta \rangle_2 + \rho_3 S_3 (T_3 - T_1) \langle \sin^3 \theta \rangle_3}{\sum_{i=1}^3 \rho_i S_i \sqrt{T_i} \langle \sin^2 \theta \rangle_i}. \quad (22)$$

We conclude that the presence of motor unit 1 slows down the systematic speed. Its single effect is the addition of an extra friction term; see the denominator in the above formula.

5. Efficiency

As pointed out in the introduction, the efficiency of a thermal motor, like the one discussed here, has to be compared with that of a Carnot engine. The fact that we can extract work by adding a load to the motor implies that there must be a concomitant transfer of energy from the hot to the cold reservoir. A fundamental difference with the Carnot construction is, however, that the motor is at all times simultaneously in contact with both the thermal reservoirs (we consider for simplicity the case of two reservoirs). As a result, we expect that the object will acquire a temperature intermediate between T_1 and T_2 . This observation is confirmed by the calculations mentioned above, where it is found that, to lowest order in ε , the velocity distribution of the motor is Gaussian at an effective temperature T_{eff} given by equation (14). At this order of perturbation, one can easily evaluate the corresponding heat flux between the reservoirs and show that it obeys a Fourier law; see below. Furthermore, it has been a matter of debate whether this irreversible entropy producing process is reducing (dramatically) the efficiency of the motor as a thermal engine. We will not discuss this matter further; see [11–13] and [4] for more details. We rather focus on a more practical definition of efficiency, namely the one considered in finite time thermodynamics. Indeed, in practical applications, Carnot efficiency is a less relevant quantity, since the central issue is not work but power. Hence, we will evaluate the efficiency of the Brownian motor at maximum power. To do so, we have to repeat the above analysis, but including an explicit calculation of the heat flux and applying a (constant) load force F to the motor.

5.1. Heat conduction

To explicitly include the energy transfer between the heat reservoirs, we add in the Boltzmann–Master equation an additional variable E_1 corresponding to the energy (change) in reservoir 1. Adding the direct acceleration produced by the external force, we obtain the following equation for the probability density $P(V, E_1, t)$ (the prime denotes pre-collisional values):

$$\begin{aligned} \partial_t P(V, E_1, t) = & \int dV' W_1(V|V') P(V', E'_1, t) - \int dV' W_1(V'|V) P(V, E_1, t) \\ & + \int dV' W_2(V|V') P(V', E_1, t) - \int dV' W_2(V'|V) P(V, E_1, t) \\ & - \frac{\partial}{\partial V} \left(\frac{F}{M} P(V, E_1, t) \right), \end{aligned} \quad (23)$$

with $W(V'|V) = \sum_i W_i(V'|V)$ the transition probability per unit time for the motor to go from speed V' to V , given by equation (3). Conservation of energy in reservoir 1 implies

$$\frac{1}{2}MV^2 + E_1 = \frac{1}{2}MV'^2 + E'_1. \quad (24)$$

For the transition probability $W_i(V; r) \equiv W_i(V'|V)$ with jump amplitude $r = V' - V$, the conservation of energy permits us to rewrite the above equation as

$$\begin{aligned} \partial_t P(V, E_1, t) &= \int dr W_1(V-r; r) P(V-r, E_1 + \frac{1}{2}Mr(2V-r), t) \\ &\quad - \int dr W_1(V; r) P(V, E_1, t) \\ &\quad + \int dr W_2(V-r; r) P(V-r, E_1, t) - \int dr W_2(V; r) P(V, E_1, t) \\ &\quad - \frac{\partial}{\partial V} \left(\frac{F}{M} P(V, E_1, t) \right). \end{aligned} \quad (25)$$

Equivalently, we have

$$\begin{aligned} \partial_t P(V, E_1, t) &= \int dr \left[e^{-r \frac{\partial}{\partial V}} e^{\frac{Mr}{2}(2V+r) \frac{\partial}{\partial E_1}} - 1 \right] W_1(V; r) P(V, E_1, t) \\ &\quad + \left[e^{-r \frac{\partial}{\partial V}} - 1 \right] W_2(V; r) P(V, E_1, t) - \frac{\partial}{\partial V} \left(\frac{F}{M} P(V, E_1, t) \right). \end{aligned} \quad (26)$$

Since $\langle E_1 \rangle = \int dV \int dE_1 E_1 P(V, E_1, t)$, the energy exchange between the reservoirs obeys the following equation:

$$\begin{aligned} \partial_t \langle E_1 \rangle &= \int dr \int dV \int dE_1 E_1 \left\{ \left[\sum_{n=0}^{\infty} \frac{(-r)^n}{n!} \frac{\partial^n}{\partial V^n} \sum_{m=0}^{\infty} \frac{(\frac{Mr}{2}(2V+r))^m}{m!} \frac{\partial^m}{\partial E_1^m} - 1 \right] W_1(V; r) \right. \\ &\quad \left. + \left[\sum_{n=0}^{\infty} \frac{(-r)^n}{n!} \frac{\partial^n}{\partial V^n} - 1 \right] W_2(V; r) - \frac{\partial}{\partial V} \frac{F}{M} \right\} P(V, E_1, t). \end{aligned} \quad (27)$$

The only non-vanishing contribution comes from the term $n = 0, m = 1$, whence

$$\partial_t \langle E_1 \rangle = - \left\langle \int dr \frac{Mr}{2} (2V+r) W_1(V; r) \right\rangle. \quad (28)$$

Using the jump moments $a_{n,i}(V)$ defined by equation (6), we can write for the heat flux from reservoir 1 to reservoir 2

$$\dot{Q}_{1 \rightarrow 2} = -\partial_t \langle E_1 \rangle = M \langle V a_{1,1}(V) \rangle + \frac{M}{2} \langle a_{2,1}(V) \rangle. \quad (29)$$

Again, the functions $a_{1,1}$ and $a_{2,1}$, see equations (9) and (10), can be expanded in terms of $\varepsilon = \sqrt{m/M}$ to find the corresponding expansion for the heat flux in the limit of large mass M . To lowest order, one finds that the energy flux obeys a Fourier law:

$$\dot{Q}_{1 \rightarrow 2} = \kappa (T_1 - T_2) + \mathcal{O} \left(\frac{1}{M^2} \right), \quad (30)$$

with

$$\kappa = \frac{k_B}{M} \frac{\gamma_1 \gamma_2}{\gamma_1 + \gamma_2}. \quad (31)$$

Table 2. Analytic result for the lowest-order contribution to the efficiency η at maximum power, in the situation of equal densities in the reservoirs ($\rho_1 = \rho_2$, $T_1 > T_2$).

Shape	Fig.	Efficiency η at maximum power
Triangula	1(a)	$\frac{\pi}{32} \frac{m}{M} (1 - \sin \theta_0)^2 \frac{(\sqrt{T_1} - \sqrt{T_2})^3}{\sqrt{T_1 T_2} (\sqrt{T_1} + \sqrt{T_2})}$
Triangulita	1(b)	$\frac{\pi}{16} \frac{m}{M} \frac{(1 - \sin^2 \theta_0)^2}{1 + \sin \theta_0} \frac{\sqrt{T_1}}{\sqrt{T_2}} \frac{T_1 - T_2}{(2\sqrt{T_1} + (1 + \sin \theta_0)\sqrt{T_2})^2}$
Triangle–triangle ($\triangleright \triangleleft$)	1(c)	$\frac{\pi}{32} \frac{m}{M} (1 - \sin \theta_0)^2 \frac{T_1 - T_2}{\sqrt{T_1 T_2}}$
Triangle–triangle ($\theta_1 \neq \theta_2$)	1(d)	$\frac{\pi}{32} \frac{m}{M} (1 + \sin \theta_1)(1 + \sin \theta_2) \frac{T_1 - T_2}{\sqrt{T_1 T_2}} \left[\frac{\sqrt{T_1}(1 - \sin \theta_2) - \sqrt{T_2}(1 - \sin \theta_1)}{\sqrt{T_1}(1 + \sin \theta_1) + \sqrt{T_2}(1 + \sin \theta_2)} \right]^2$

5.2. Power

The time evolution for the average speed obtained from the Boltzmann equation (23),

$$\partial_t \langle V \rangle = \langle a_1(V) \rangle + \frac{F}{M}, \tag{32}$$

differs from equation (7) by the acceleration resulting from the addition of the force F . To lowest order in ε , the steady-state solution of equation (8) for the second moment is unaffected by F (i.e., $M \langle V^2 \rangle = k_B T_{\text{eff}}$) and we find that

$$\langle a_1(V) \rangle = -\frac{\gamma}{M} (\langle V \rangle - V_0). \tag{33}$$

Here γ is the friction coefficient, see equation (12), and V_0 the average steady-state velocity in the absence of an external force; see equation (15). The steady-state solution of equation (32) thus reads

$$\langle V \rangle = V_0 + \frac{F}{\gamma}. \tag{34}$$

Note that $F_{\text{stop}} = -\gamma V_0$ is the stopping force (at this order of perturbation). Obviously, in order to extract work from the Brownian motor we need to apply a force smaller than F_{stop} . In particular one has that $F \sim 1/M$.

One defines the efficiency of the motor as the delivered work per unit time over the heat exchange per unit time (for simplicity, we assume from here on that $T_1 > T_2$):

$$\eta = \frac{P}{\dot{Q}_{1 \rightarrow 2}} = \frac{-F \langle V \rangle}{\dot{Q}_{1 \rightarrow 2}}. \tag{35}$$

Since to lowest order of the perturbation in ε the heat flux is not influenced by an external constant force F , we can maximize the efficiency by maximizing the power $-F \langle V \rangle$. One easily verifies that the latter is maximal when we apply a force equal to half the stopping force, $F = -\gamma V_0/2$. The resulting efficiency of the thermal engine at maximum power is then given by

$$\eta = \frac{M}{4k_B} \frac{(\gamma_1 + \gamma_2)^2}{\gamma_1 \gamma_2} \frac{V_0^2}{T_1 - T_2}. \tag{36}$$

One can immediately deduce from equations (12) and (15) that the efficiency η is very low, due to a prefactor m/M : for small m/M the heat conductivity is the dominant factor and both the rectified motion and resulting work are a second-order effect. This observation is of course restricted to our discussion of the small- ε limit. In fact much higher efficiencies can be in principle be achieved when one moves away from this limit [14].

Since the expression for the efficiency of an arbitrary motor, equation (36), is rather complex, we have reproduced the efficiency for the models of figure 1 in table 2. In particular, η simplifies significantly for identical conditions in both reservoirs (equal densities $\rho_1 = \rho_2$ and equal objects $F_1(\theta) = F_2(\theta)$ and $S_1 = S_2$):

$$\eta = \frac{\pi}{32} \frac{m}{M} \left(\frac{\langle \sin^3 \theta \rangle}{\langle \sin^2 \theta \rangle} \right)^2 \frac{(\sqrt{T_1} - \sqrt{T_2})^3}{\sqrt{T_1 T_2} (\sqrt{T_1} + \sqrt{T_2})}. \quad (37)$$

References

- [1] Reimann P 2002 *Phys. Rep.* **361** 57
- [2] Reimann P, Kawai R, Van den Broeck C and Hänggi P 1999 *Europhys. Lett.* **45** 545
Jülicher F and Prost J 1995 *Phys. Rev. Lett.* **75** 2618
- [3] Parrondo J M R and Jiménez de Cisneros B 2002 *Appl. Phys. A* **75** 193
- [4] Van den Broeck C, Kawai R and Meurs P 2004 *Phys. Rev. Lett.* **93** 090601
Van den Broeck C, Meurs P and Kawai R 2005 *New J. Phys.* **7** 10
- [5] Meurs P, Van den Broeck C and Garcia A 2004 *Phys. Rev. E* **70** 051109
- [6] von Smoluchowski M 1912 *Z. Phys.* **13** 1069
- [7] Feynman R P, Leighton R B and Sands M 1963 *The Feynman Lectures on Physics I* (Reading, MA: Addison-Wesley) chapter 46
- [8] Van Kampen N G 1981 *Stochastic Processes in Physics and Chemistry* (Amsterdam: North-Holland)
- [9] Onsager L 1931 *Phys. Rev.* **37** 405
Onsager L 1931 *Phys. Rev.* **38** 2265
- [10] Gomez-Marin A and Sancho J M 2005 *Phys. Rev. E* **71** 021101
- [11] Parrondo J M R and Espagnol P 1996 *Am. J. Phys.* **64** 1125
- [12] Jarzynski C and Mazonka O 1999 *Phys. Rev. E* **59** 6448
- [13] Sokolov I M 1999 *Europhys. Lett.* **44** 278
- [14] Van den Broeck C 2005 Thermodynamic efficiency at maximum power *Phys. Rev. Lett.* submitted